J Biochem Tech (2018) Special Issue (2): 72-80
ISSN: 0974-2328

Study of Binding Energies of the Deformed $^{230-238}$U Isotopes Using the Skyrme Force

M. R. Pahlavani *, H. Babazadeh

Received: 25 February 2018 / Received in revised form: 25 May 2018, Accepted: 29 May 2018, Published online: 05 September 2018

Abstract

The Thomas-Fermi energy density formalism is employed to study the binding energy of $^{230-238}$U Uranium isotopes. Total binding energies of deformed $^{230-238}$U isotopes are studied considering the quadrupole β2 and the hexadecapole β4 deformation parameters. The total Thomas-Fermi energy is minimized with respect to deformation in order to obtain the accurate binding energies of the $^{230-238}$U isotopes. Calculated binding energies using the present studies are compared with the available experimental data. Well agreement achieved between the calculated and the experimental data. Difference between the calculated average binding energies and experimental data was obtained less than 0.01 MeV.

Keywords: Skyrme interaction; Binding energy; Coulomb interaction; quadrupole and hex-adecapole deformation; Uranium isotopes

PACS numbers: 21.10.Dr, 21.65.Ef, 21.10.S

Introduction

A fundamental aspect of theoretical nuclear physics is the study of the structure of finite nucleiin terms of the nucleon-nucleon interaction. The binding energy is proof for the stability of everyfinite systems such nuclei. Initial attempts to study nuclear binding energy and its stability werecarried out using macroscopic approaches such as the semi-empirical liquid drop model (LDM) (Bao-Qiu and et al, 2004) and semi-classical Thomas-Fermi energy density functional model (TFEDFM) (Centelles and et al, 2007; Mayers and et al, 2009). In theLDM, the binding energy and the mass of a nucleus can be written as the summation of adjustableparameters (coefficients of the volume energy, the symmetry energy, the incompressibility and thesurface energy). The LDM describes very well the average trends of nuclear binding energy (Mackie. And et al, 1977; Audi & Wapstra, 1993). These coefficients can be calculated by fitting to the experimentally known masses of some nuclei.Quantum mechanical microscopic models such as the Hartree-Fock mean field (Stone, 2005) and the relativistic Dirac-Bruckner-Hartree-Fock models, DBHF, (Sammarruca and et al, 2010; Van Giai and et al, 2010) with suitable potential have also been employed to study the properties and structure of the finite nuclei. The mean field Hartree-Fock model uses of the nucleons is relatively low and the interaction between nucleons is relatively weak, making the nucleon-nucleon correlation small. The Hartree-Fock mean field theory is a major theoretical tool for dealing with systems with little correlation. It produces the appropriate single-particle potential corresponding to the actual density distribution for a given nucleus. This corresponds to an effective energy-density functional because nuclei are made from two types of particles (neutrons and protons) and the nucleon-nucleon interaction is an approximated concept which is harder tounderstand than the electronic structure of atoms. Most fundamental models use the interaction

between nucleons as input (Machleidt & Slaus, 2001) and calculate the equation of state using nuclear matter diagrammatictechniques (Kaiser and et al, 2002; Fogaça & Navarra, 2006). These microscopic models have made good progress (Navrátil and et al, 2012; Pieper and et al, 2004). Some carry outcalculations for finite nuclei in a no-core shell model, a coupled cluster (Włoch and et al, 2005; Nie, 2007) or using the unitarycorrelation method (Roth and et al, 2005). The shell corrections for the microscopic-macroscopic (mic-mac) approachhave also been very successful in reproducing the systematic of the known nuclear binding energy (Aboussir and et al, 1995). Mic-mac methods depend strongly on phenomenological information. When one extrapolatesmagic nuclei, doubts may arise from the

M. R. Pahlavani *, H. Babazadeh
Department of nuclear physics, Faculty of Basic science,University of Mazandaran, P.O.Box 47415-416, Babolsar, Iran

***Email:** Hikmat_alnassir10 @ yahoo.com

use of the Nilsson or Yukawa potential which is added as independent additional information that is not self-consistent. The consideration of two, three or more nucleon interactions leads to the so-called ab - initio method (Karki and et al, 1997; Nakamura and et al, 2008; Vary and et al, 2009; Pickard & Needs, 2011) that consists of solving the nuclear many-body problem using numerical methods as exactly as possible. Recently, in particle physics, the one Boson exchange potential has been developed to obtain the binding energies of light nuclei such as in the AdS/CFT and AdS/QCD approaches (Pahlavani and et al, 2010; Pahlavani and et al, 2011; Pahlavani & Morad, 2013). Despite these efforts, their accuracy remains limited.The three excellent methods for explaining nuclear properties are the Skyrme energy functional,which is zero range and density dependent, the Skyrme-Hartree-Fock (SHF) model (Rashdan, 2000; Karataglidis and et al, 2010) and the relativistic mean field model (Dutra and et al, 2014; Miyatsu and et al, 2015). Self-consistent mean field models fall between the ab-initio method and the mic-mac method. The connection between the ab - initio and the SHF models is still under development (Brack and et al, 1985). Although the ab - initio type approaches have shown significant progress, they remain limited to the light nuclei with small mass numbers. A developed version of this type is the extended Thomas-Fermi-Skyrme interaction model (Bartel and et al, 2008). Since the original work by Skyrme in the 1950s (Skyrme, 1956) and the Vautherin and Brink (Vautherin, 1972) parametrization of the original interaction in the early 1970s, considerable effort has been invested in the application of this density- dependent effective interaction to both ground-state properties of finite nuclei and nuclear matter in the framework of the mean-field Hartree-Fock approximation (Bender and et al, 2003; Stone and et al, 2016). The advantage of the structure of the Skyrme density functional is that it allows analytical expression of all variables characterizing infinite nuclear matter (Chabanat and et al, 1997; Dutra and et al, 2008). The Skyrme energy density functional model is able to reproduce quite accurate experimental data on binding energy and nuclear decay barriers such as fusion, fission and cluster decay barriers. The theory presented by Brueckner et al. (Brueckner and et al, 1954), established an essential framework which, in principle,relates the nuclear structure to the two-nucleon interactions. However, previous attempts have failed to reproduce binding energies with reasonable accuracy, single-particle energies, and charge-density distributions for the finite nuclei. The empirical value of E_0 per nucleon of about 16 MeV can be extracted from a semi-empirical mass formula or from the extrapolation of the binding energies of the heavy nuclei (Basu, 2005).Various many-body techniques typically lead to over-estimation of the saturation density ρ_0 of the symmetric nuclear matter at which the binding energy per nucleon reaches its maximum (Li, and et al, 2006).The nuclear deformation includes a wide range of nuclei from the light to the super heavy. The heavy and superheavy nuclei are not spherical and it is essential to take into account the nuclear deformation, including the quadrupole, the hexadecapole and the hexacontatrapole deformations,in the theoretical calculation. In this study, our claim is to investigate the role of the deformation effects on the effective potential and total binding energy. Various many-body techniques typically lead to an over estimations of the saturation density ρ_0 of symmetric nuclear matter SNM, at which the binding energy per nucleon (average binding energy) reaches its maximum (Li, and et al, 2006).section2 gives a brief description of semiclassical expression of the Skyrme energy density functional.The results of the calculations for binding energy with respect to deformations are presented in Section3. Finally, a summary of the investigation is given in section4.

Skyrme density functional approach

The Skyrme force was first introduced by Skyrme (Skyrme, 1958) as an effective force for the nuclear Hartree-Fock calculations. Corresponding to the density functional theory, the energy density functional depends on the densities and currents (and their derivatives) representing the distributions of nucleonic matter, the spins, the momenta and the kinetic energy. The SHF framework has been successful in reproducing the nuclear matter related to the finite nuclei (Dutra and et al, 2008) and the Skyrme effective interaction has been extensively applied to reproduce the nuclear properties and decay. There is some evidence for employing the SHF model to study the hyper-nuclei properties. During the development of the SHF theory, many parameter sets were proposed to reproduce the properties of nuclear matter and the finite nuclei. The total energy in the Skyrme energy density functional approach can be calculated using (41):

$$H(r) = k + H_0 + H_3 + H_{fin} + H_{eff} + Hso + Hsg + H_{coul} \qquad (1)$$

where H(r) is the energy density functional, E_k is the density of the kinetic energy, H0 is the zero range energy, H3 is the density-dependent term, H_{eff} is the finite range term, H_{so} is the spin-orbit coupling energy, H_{coul} is the Coulomb energy with the exchange corrections and H_{sg} is the coupling between the spin and gradient, which is small and neglected in many calculations. The general energy density formula is as follows:

$$H(r) = C_k(\rho_q)^{5/3} + \frac{1}{4}\ \text{to}\ [(2 + \text{Xo})\ \rho^2 - (2\text{xo} + 1)\ (\rho_p^{\ 2} + \rho_n^{\ 2})]$$

$$+\frac{1}{24} t_3 \rho^{\alpha}(2 + x_3)\rho^2 \_ (2x_3 + 1)(\rho_p^{\ 2} + \rho_n^{\ 2})] + \frac{1}{8}\ [\ t_1\ (2+x_1) + t_2(2+x_2)\big]\tau\rho$$

$$+\frac{1}{8}\,[t_2\,(2x_2+1)-t_1(2x_1+1)]\,(\tau_p\rho_p+\tau_p\rho_n)+\frac{1}{32}\,[3t_1\,(2+x_1)-t_2\,(2+x_2)]\,(\nabla p)^2$$

$$-\frac{1}{32}\,[3t_1(2x_1+l)+t_2(2x_2+l)]\,[(\nabla\rho_p)^2+(\nabla\rho_n)^2]+\frac{1}{2}\,Wo\,[J.\nabla\rho+J_p.\nabla\rho_p+J_n.\nabla\rho_n]$$

$$-\frac{1}{16}(t_1x_1+t_2x_2)\,J^2+\frac{1}{16}\,(t_1-t_2)\left[J_p^{\,2}+J_n^{\,2}\right] \qquad (2)$$

In which the total density can be described as the summation of the neutron and proton densi ties. Total density, kinetic energy and angular momentum are the sum of the proton and neutron
Contributions as:

$$\rho=\rho_n+\rho_p \quad \tau=\tau_n+\tau_p \quad J=J_n+J_p \qquad (3)$$

Where n and p denote neutron and proton, respectively. As stated earlier, different formalisms exist

With different numbers of adjustable parameters. Great effort has been made to investigate the properties of nuclei and the results of different sets of parameters (Stone, 2007). The energy density function used in this investigation includes ten parameters (Chabanat and et al, 2007; Chabanat and et al, 2008). Adjustable parameters can be obtained using fitting to the known experimental or theoretical data of a nucleus with acceptable accuracy.The values of these parameters play important roles in obtaining favorable results (Gupta and et al, 2009). In our calculation, the macroscopic energy is calculated using the Skyrme interaction with parameter set SkM.

Results and Discussion

The goal of the current study was to calculate the binding energy using the Skyrme energy density function presented in Equation (1) considering the deformation. The Coulomb part of energy for the density of the energy function can be calculated as:

$$v_c(r)=if\ \begin{cases} r\geq R_c \rightarrow \dfrac{1}{4\pi\varepsilon_0}\dfrac{ze^2}{R_c^{\,2}} \\ r\leq R_c \rightarrow \dfrac{1}{4\pi\varepsilon_0}\dfrac{ze^2}{R_c^{\,2}}\left(3-\dfrac{r^2}{R_c^{\,2}}\right) \end{cases} \qquad (4)$$

where Rc is the radius of the charge distribution.

$$Ecoul=\frac{e^2}{2}\int d^3r\,d^3r'\,\frac{\rho(r)\rho(r')}{|r-r'|}-\frac{3e^2}{4}\left(\frac{3}{\pi}\right)^{1/3}\int d^3r\,\left[\rho(r)\right]^{4/3} \qquad (4)$$

The density used in Equation (12) is only proton density. The second part of this equation corresponds to the exchange correlation in which the Pauli Exclusion Principle has taken in to account. The total energy density function includes both the density of the neutrons and protons. There are many types of energy density functions. In these calculations, the two-parameter Fermi density distribution was used for the proton and neutron density

$$\rho(r)=\frac{\rho_0}{1+\exp(\dfrac{r-R_q}{a_q})} \qquad (5)$$

Where ρ_0 and aq are adjustable parameters of the distribution and are different for the neutrons and protons in each nucleus. Parameter $\rho 0$ is the saturation density and is calculated by normalizingthe proton number density function to atomic number Z and the neutron number density functionto N for each known nucleus. R is the nuclear radius and is the diffuseness thickness parameter.In this model, the binding energy is obtained by integrating over the full range of radius variabler.

$$E = \int H(r) d^3 r \quad (6)$$

The distribution of neutrons and protons inside the nucleus follows a two-parameter Fermi density function. However, it should be noted that parameters within the two-parameter relationship are different for neutrons and protons. In order to obtain the saturation densities, the density is normalized relative to the number of nucleons (neutrons and protons),

$$\int_0^\infty \rho_{p,n}(r) d^3 r = Z : N \quad (7)$$

Since the radius of the deformed nuclei is a function of the angle, the radius is obtained from the Following expansion

$$\mathrm{R}(\theta,\phi) = \mathrm{R}_0 (1 + \sum_{l,m} \beta_{l,m} Y_{l,m}(\theta,\phi)) \quad (8)$$

Therefore, the density and radius of the nucleus also varied with the angle φ. This in turn causes a variation in the calculation of the nuclear interaction potential. In the above relation, $\beta_{l,m}$ and $Y_{l,m}$ are in order, the deformation parameter and spherical harmonic. By considering the quadrupole deformation with axial symmetry relative to the angle', it yield

$$\rho_i(\mathrm{r}) = \rho_{0i} / (1 + \exp(\tfrac{(r - R(\theta,\varphi))}{a}) \quad (9)$$

In order to obtain ρ_0 (ρ_{0p} or ρ_{0N}) for the deformed nucleus, the following normalization conditions

are applied,

$$\rho 0i = \frac{(Z:N)}{2\pi \int_0^\pi \int_0^{R(\theta)} \rho_i(r,\theta) r^2 \sin(\theta) d\theta}$$

$$2\pi\rho_{0i} \int_0^\pi \sin(\theta) d\theta \int_0^R 1 \Big/ (1 + \exp\left(\frac{(r-R)}{a}\right) r^2 dr$$

And after a radial integration, one obtains

$$\begin{aligned} &\int_0^R \frac{r^2 dr}{1+\exp\left(\frac{(r-R)}{a}\right)} = R^3/3 + 2a^3(-1 + \frac{1}{8} - \frac{1}{27} + \frac{1}{58} \cdots) \\ &-2a^2 R(-1 + \frac{1}{4} - \frac{1}{9} + \frac{1}{16} - \frac{1}{25} \cdots) \\ &-2a^3(-\frac{1}{\exp(\frac{R}{a})} + \frac{1}{\exp(\frac{2R}{a})} - \frac{1}{\exp(\frac{3R}{a})} + \cdots) - aR^2 log(2) \end{aligned} \quad (10)$$

Taking into account the two-parameter Fermi density distribution and by considering deformation and relying on it, in relation to the energy density and integration over it in all space, saturation density is obtained for different isotopes. Table 2. Presents a comparison of the results of the calculation with the results of the spherical shape.

Table 1: Values of deformation parameter β2, and β4 for nuclei (Möller and et al, 2016)

nuclei	β_2	β_4
^{230}U	0.185	0.126
^{231}U	0.195	0.114
^{232}U	0.206	0.116

^{233}U	0.206	0.116
^{234}U	0.215	0.106
^{235}U	0.215	0.106
^{236}U	0.226	0.108
^{237}U	0.226	0.095
^{238}U	0.236	0.095

Table 2: Saturation densities of uranium isotopes in terms of (fm-3) for spherical and deformed states

nuclei	ρ_{0n} (spherical)	ρ_{0p} (spherical)	ρ_0 (spherical)	ρ_{0n} (deformed)	ρ_{0p} (deformed)	ρ_0 (deformed)
^{230}U	0.0900	0.0615	0.1515	0.0911	0.0607	0. 1518
^{231}U	0.0902	0.0612	0.1514	0.0912	0.0604	0.1516
^{232}U	0.0904	0.0610	0.1514	0.0914	0.0601	0.1514
^{233}U	0.0905	0.0608	0.1513	0.0916	0.0598	0.1514
^{234}U	0.0908	0.0606	0.1513	0.0918	0.0595	0.1513
^{235}U	0.0909	0.0603	0.1512	0.0920	0.0592	0.1512
^{236}U	0.0911	0.0602	0.1513	0.0922	0.0589	0.1510
^{237}U	0.0912	0.0599	0.1512	0.0924	0.0586	0.1510
^{238}U	0.0917	0.0595	0.1513	0.0927	0.0580	0.1508

Table 2 shows that the central density decreases with increasing mass and atomic number. Using the results of Table 2 and taking into account deformation in the density distribution function and By integration of the energy density, the average binding energy of these isotopes were calculatedand compared with experimental data in Table 3

Table 3: Calculated average binding energy using the present approach for spherical and deformed uranium isotopes compared with experimental data.

nuclei	Average binding energy,Mev (spherical)	Average binding energy,Mev (deformed)	Average binding energy,Mev (experimental)
^{230}U	7.6273	7.6208695	7.62086
^{231}U	7.6203	7.6160173	7.61125
^{232}U	7.6253	7.616681	7.61163
^{233}U	7.6172	7.605458	7.60386
^{234}U	7.6174	7.60555	7.60042
^{235}U	7.6018	7.593617	7.590638
^{236}U	7.6029	7.593701	7.58644
^{237}U	7.5894	7.58059	7.57594
^{238}U	7.5893	7.5806	7.570217

Conclusion

The current study focused on calculating the binding energy of even-even, even-odd and odd-oddUranium isotopes using the Skyrme effective interaction, considering the quadrupole and hexadecapole deformations. In order to calculate the nuclear average binding energies, the two parameter Fermi density distribution, the nucleon radius and saturation density were employed. The results obtained

using the present approach are in good agreement with the available experimental data. Using the present approach and considering quadrupole and hexadecapole deformations, the total and the average binding energies of the Uranium isotopes were calculated. The results show that with the addition of deformation (both for positive and negative deformation parameters), the value of the binding energy decreased and became closer to the experimental data. Although the quadrupole deformation is more effective compared to the hexadecapole deformation, the hexadecapole coeffcient is not ignored in the calculations of the nuclear binding energy. Within this semi-microscopic approach, it is possible to calculate the binding energy with high accuracy without having to go through the full self-consistency HF approach.

References

Aboussir, Y., Pearson, J. M., Dutta, A. K., & Tondeur, F. (1995). At. Data Nucl. Data Tab. 61: 127 (1995). *Möller P, Nix JR, Myers WD, Swiatecki WJ. At. Data Nucl. Data Tab*, *59*, 185.

Audi, G., & Wapstra, A. H. (1993). The 1993 atomic mass evaluation:(I) Atomic mass table. *Nuclear Physics A*, *565*(1), 1-65.

Bao-Qiu, C. H. E. N., & Zhong-Yu, M. A. (2004). Fusion barrier of super-heavy elements in a generalized liquid drop model. *Communications in Theoretical Physics*, *42*(4), 594.

Bartel, J., Bencheikh, K., & Meyer, J. (2008). Extended Thomas-Fermi density functionals in the presence of a tensor interaction in spherical symmetry. *Physical Review C*, *77*(2), 024311.

Basu, D. N. (2005). Equation of state for nuclear matter based on density dependent effective interaction. *International Journal of Modern Physics E*, *14*(05), 739-749.

Bender, M., Heenen, P. H., & Reinhard, P. G. (2003). Self-consistent mean-field models for nuclear structure. *Reviews of Modern Physics*, *75*(1), 121.

Brack, M., Guet, C., & Hakansson, H. B. (1985). Selfconsistent semiclassical description of average nuclear bulk properties-a link between microscopic and macroscopic models. *Physics Reports*, *123*, 275-364.

Brueckner, KA, Levinson, CA, & Mahmoud, HM (1954). Two-body forces and nuclear saturation. I. Central forces. *Physical Review* , *95* (1), 217.

Centelles, M., Schuck, P., & Vinas, X. (2007). Thomas–Fermi theory for atomic nuclei revisited. *Annals of Physics*, *322*(2), 363-396.

Chabanat, E., Bonche, P., Haensel, P., Meyer, J., & Schaeffer, R. (1997). A Skyrme parametrization from subnuclear to neutron star densities. *Nuclear Physics A*, *627*(4), 710-746.

Chabanat, E., Bonche, P., Haensel, P., Meyer, J., & Schaeffer, R. (1997). A Skyrme parametrization from subnuclear to neutron star densities. *Nuclear Physics A*, *627*(4), 710-746.

Chabanat, E., Bonche, P., Haensel, P., Meyer, J., & Schaeffer, R. (1998). A Skyrme parametrization from subnuclear to neutron star densities Part II. Nuclei far from stabilities. *Nuclear Physics A*, *635*(1-2), 231-256.
Gupta, R. K., Singh, D., Kumar, R., & Greiner, W. (2009). Universal functions of nuclear proximity potential for Skyrme nucleus–nucleus interaction in a semiclassical approach. *Journal of Physics G: Nuclear and Particle Physics*, *36*(7), 075104.

Dutra, M., Lourenço, O., Avancini, S. S., Carlson, B. V., Delfino, A., Menezes, D. P., ... & Stone, J. R. (2014). Relativistic mean-field hadronic models under nuclear matter constraints. *Physical Review C*, *90*(5), 055203.

Dutra, M., Lourenco, O., Delfino, A., Martins, J. S., Providencia, C., Avancini, S. S., & Menezes, D. P. (2008). Skyrme forces versus relativistic models: Reexamining instabilities. *Physical Review C*, *77*(3), 035201.

Fogaça, D. A., & Navarra, F. S. (2006). Solitons in relativistic mean field models. *Physics Letters B*, *639*(6), 629-634.

Kaiser, N., Fritsch, S., & Weise, W. (2002). Nuclear mean field from chiral pion–nucleon dynamics. *Nuclear Physics A*, *700*(1-2), 343-358.

Karataglidis, S., Henninger, K. R., Richter, W. R., & Amos, K. (2010). Proton scattering observables from Skyrme-Hatree-Fock densities. *arXiv preprint arXiv:1008.1676*.

Karki, B. B., Stixrude, L., Clark, S. J., Warren, M. C., Ackland, G. J., & Crain, J. (1997). Structure and elasticity of MgO at high pressure. *American Mineralogist*, *82*(1-2), 51-60.

Li, ZH, Lombardo, U., Schulze, HJ, Zuo, W., Chen, LW, & Ma, HR (2006). Nuclear matter saturation point and symmetry energy with modern nucleon-nucleon potentials. *Physical Review C* , *74*(4), 047304.

Machleidt, R., & Slaus, I. (2001). The nucleon-nucleon interaction. *Journal of Physics G: Nuclear and Particle P*

Mackie, F. D., & Baym, G. (1977). Compressible liquid drop nuclear model and mass formula. *Nuclear Physics A*, *285*(2), 332-348.

Miyatsu, T., Cheoun, M. K., & Saito, K. (2015). Equation of State for Neutron Stars With Hyperons and Quarks in the Relativistic Hartree–fock Approximation. *The Astrophysical Journal*, *813*(2), 135.

Möller, P., Sierk, A. J., Ichikawa, T., & Sagawa, H. (2016). Nuclear ground-state masses and deformations: FRDM (2012). *Atomic Data and Nuclear Data Tables*, *109*, 1-204.

Myers, W. D., & Świątecki, W. J. (1999). Thomas-Fermi fission barriers. *Physical Review C*, *60*(1), 014606.

Nakamura, H., Yamashita, K., Rocha, A. R., & Sanvito, S. (2008). Efficient ab initio method for inelastic transport in nanoscale devices: Analysis of inelastic electron tunneling spectroscopy. *Physical Review B*, *78*(23), 235420.

Navrátil, P., Vary, J. P., & Barrett, B. R. (2000). Large-basis ab initio no-core shell model and its application to 12 C. *Physical Review C*, *62*(5), 054311.

Nie, G. K. (2007). Specific Density Of Binding Enerfy Of Core In Beta-Stable Nuclei is 2.57 MeV/fm^ 3. *arXiv preprint arXiv:0707.4291*.

Pahlavani, M. R., & Morad, R. (2013). Binding energy of light nuclei using the noncritical holography model. *Physical Review C*, *88*(6), 064004.

Pahlavani, M. R., Sadeghi, J., & Morad, R. (2010). Binding energy of a holographic deuteron and tritium in anti-de-Sitter space/conformal field theory (AdS/CFT). *Physical Review C*, *82*(2), 025201.

Pahlavani, M. R., Sadeghi, J., & Morad, R. (2011). Holographic 3He and 4He nuclei. *Journal of Physics G: Nuclear and Particle Physics*, *38*(5), 055002.

Pickard, C. J., & Needs, R. J. (2011). Ab initio random structure searching. *Journal of Physics: Condensed Matter*, *23*(5), 053201.

Pieper, S. C., Wiringa, R. B., & Carlson, J. (2004). Quantum Monte Carlo calculations of excited states in A= 6–8 nuclei. *Physical Review C*, *70*(5), 054325.

Rashdan, M. (2000). A Skyrme parametrization based on nuclear matter BHF calculations. *Modern Physics Letters A*, *15*(20), 1287-1299.

Roth, R., Hergert, H., Papakonstantinou, P., Neff, T., & Feldmeier, H. (2005). Matrix elements and few-body calculations within the unitary correlation operator method. *Physical Review C*, *72*(3), 034002.

Sammarruca, F., Chen, B., Coraggio, L., Itaco, N., & Machleidt, R. (2012). Dirac-Brueckner-Hartree-Fock versus chiral effective field theory. *Physical Review C*, *86*(5), 054317.

Skyrme, T. H. R. (1956). CVII. The nuclear surface. *Philosophical Magazine*, *1*(11), 1043-1054.

Skyrme, T. H. R. (1958). The effective nuclear potential. *Nuclear Physics*, *9*(4), 615-634.

Stone, J. R. (2005). Self-consistent Hartree–Fock mass formulae: a review. *Journal of Physics G: Nuclear and Particle Physics*, *31*(11), R211.

Stone, J. R. (2007). JR Stone and P.-G. Reinhard, Prog. Part. Nucl. Phys. 58, 587 (2007). *Prog. Part. Nucl. Phys.*, *58*, 587.

Stone, J. R., Guichon, P. A. M., Reinhard, P. G., & Thomas, A. W. (2016). Finite nuclei in the quark-meson coupling model. *Physical review letters*, *116*(9), 092501.

Van Giai, N., Carlson, B. V., Ma, Z., & Wolter, H. (2010). The Dirac–Brueckner–Hartree–Fock approach: from infinite matter to effective Lagrangians for finite systems. *Journal of Physics G: Nuclear and Particle Physics*, *37*(6), 064043.

Vary, J. P., Maris, P., Ng, E., Yang, C., & Sosonkina, M. (2009). Ab initio nuclear structure–the large sparse matrix eigenvalue problem. In *Journal of Physics: Conference Series* (Vol. 180, No. 1, p. 012083). IOP Publishing.

Vautherin, D. (1972). D. Vautherin and DM Brink, Phys. Rev. C 5, 626 (1972). *Phys. Rev. C*, *5*, 626.

Włoch, M., Dean, D. J., Gour, J. R., Hjorth-Jensen, M., Kowalski, K., Papenbrock, T., & Piecuch, P. (2005). Ab-Initio Coupled-Cluster Study of O 16. *Physical review letters*, *94*(21), 212501.

Xu, Y., Guo, H., Han, Y., & Shen, Q. (2013). New Skyrme interaction parameters for a unified description of the nuclear properties. *Journal of Physics G: Nuclear and Particle Physics*, *41*(1), 015101.

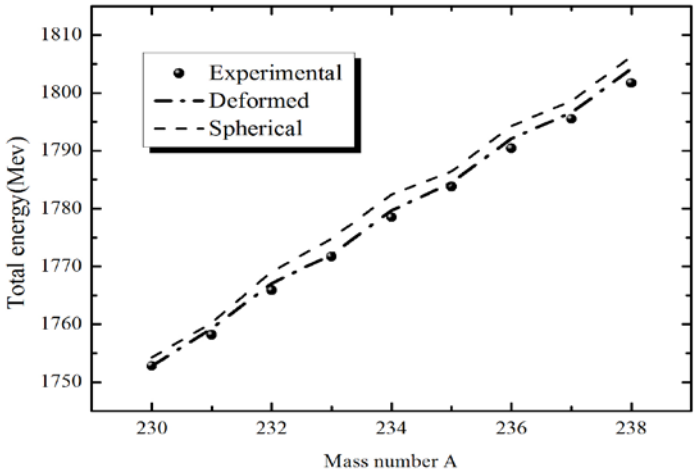

Fig. 1: Total binding energy for Uranium isotopes compared with experimental data and deformations.

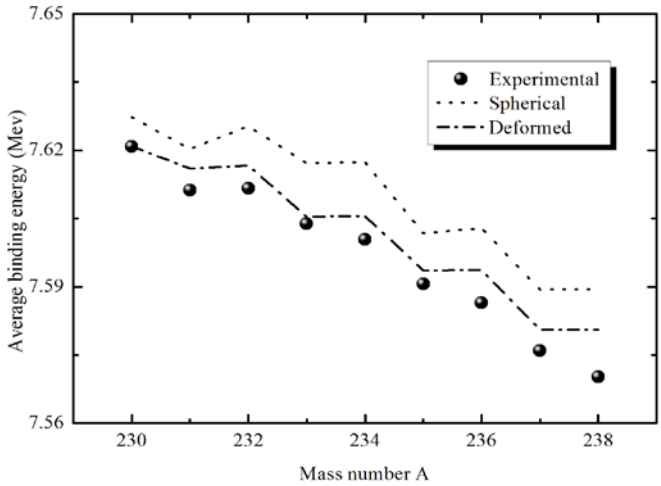

Fig. 2: Average binding energy for Uranium isotopes compared with experimental data and

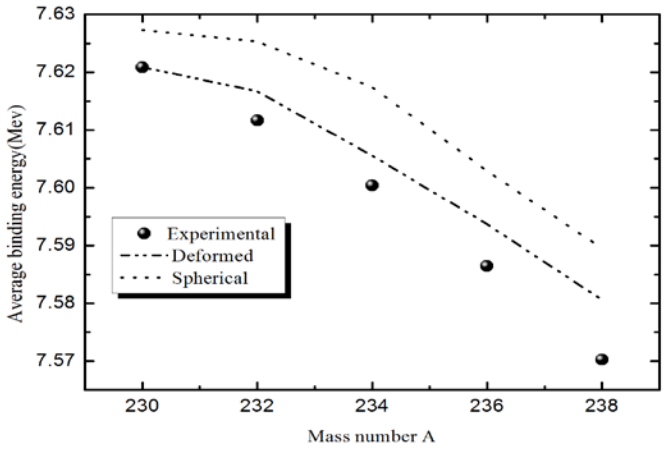

Fig. 3: Average binding energy for even isotopes compared with experimental data with defor-mations.

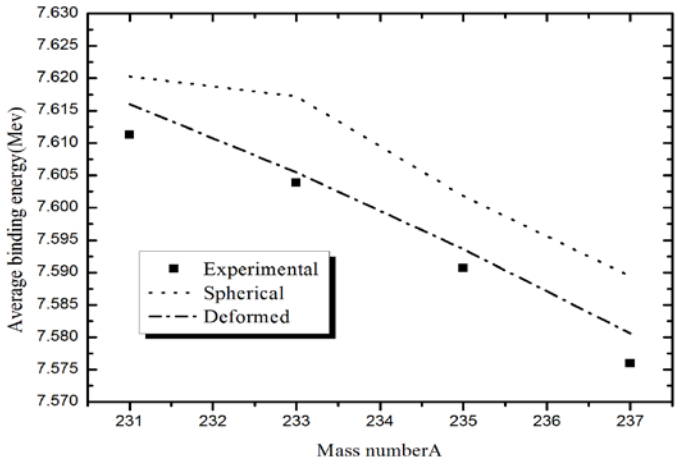

Fig. 4: Average binding energy for odd isotopes compared with experimental data with defor- mations